Mini Review

International Journal of Dental Research and Oral Health

The Ingrained Foible-Stafne Bone Defect

Anubha Bajaj*

Histopathologist in A.B. Diagnostics, New Delhi, India.

Correspondence author*

Anubha Bajaj
Histopathologist in A.B. Diagnostics
New Delhi
India

Submitted : 24 Jun 2022 ; Published : 11 July 2022

Citation: Bajaj, A. The Ingrained Foible-Stafne Bone Defect. J Dental Oral Health, 2022; 4(2): 1-4.

Preface: Stafne bone defect is a cortical bone defect emerging adjacent to angle of the mandible beneath the mandibular canal. The lesion represents a depression within medial aspect of mandible and is generally imbued with a portion of submandibular gland or mature adipose tissue. Stafne bone defect was initially characterized as a mandibular depression by Edward Stafne in 1942 (Stafne, 1942).

The condition appears as an incidental finding and is additionally designated as Stafne bone cavity, Stafne bone cyst, static bone cavity of the mandible, lingual salivary gland depression, lingual mandibular bone depression, lingual salivary gland inclusion defect, developmental salivary gland defect, Stafne defect, static bone cavity, latent bone cyst, mandibular salivary gland defect, idiopathic bone cavity, developmental bone defect of the mandible or ectopic salivary gland.

The lesion is incorporated with salivary gland tissue, lymphoid tissue, skeletal muscle, soft tissue, mature adipose tissue or vascular tissue and may be coined with contemporary terms as “benign mandibular concavity”.Besides, the bone defect is essentially devoid of accumulated fluid and the lesion may not be contemplated as a cyst. Panoramic radiograph is necessitated to obtain an overview of dento-maxillofacial complex, pertinent anatomical landmarks, boundaries of adjacent structures and associated pathology within the jaws. However, aberrant anatomical configuration and accompanying radiographic features may ensure a misinterpretation of the lesion as a pathological disorder or an odontogenic lesion.

Disease Characteristics: Stafne bone defect is frequently encountered in middle aged subjects. A male predominance is delineated. The condition is commonly discerned in adults above > 50 years and generally occurs within the fifth decade or sixth decade (Morita et al., 2021; Aps et al., 2020). Stafne bone defect is categorized into

- lingual posterior
- lingual anterior
- lingual ramus or
- buccal ramus.

Upon radiographic disease discernment, estimated disease prevalence varies from 0.10% to 0.48% whereas incidence of posterior lingual variant appears at below <0.5%. In contrast, anterior lingual variant is minimally prevalent as the lesion emerges between incisors and premolar area, superior to insertion of mylohyoid muscle (Morita et al., 2021; Aps et al., 2020). Of obscure aetiology, Stafne bone defect is posited to engender bony depression due to lobar hypertrophy of a salivary gland and bony erosion occurring on account of aberrant vascular pressure or vascular compression from diverse vascular articulations or incomplete calcification of Meckel cartilage during ossification (Morita et al., 2021; Aps et al., 2020). Stafne bone defect possibly ensues due to bone remodelling on account of adjacent salivary gland tissue. The defect may retrogress following resection of abutting salivary gland. Generally, the bone defect is encountered between first molar of the mandible and mandibular angle. However, the established “glandular hypothesis” postulates that the bony cavity is configured due to pressure exerted by a hyperplastic glandular lobe of submandibu submandibular, sublingual or parotid salivary gland confined within the lingual cortex of mandible for a significant duration (Morita et al., 2021; Aps et al., 2020).

Clinical Elucidation: Stafne bone defect may emerge as an asymptomatic, incidental radiographic feature within the mandible. Stafne bone defect is frequently located upon the lingual margin of posterior mandibular region, concordant to submandibular gland. Lingual anterior Stafne bone defect usually emerges within the region of premolars and canines and can be misinterpreted as a cystic lesion. Besides, Stafne bone defect can arise within the lingual ramus and buccal ramus (Kaya et al., 2018; Hisatomi et al., 2019).

Exceptionally, the depression appears within mandibular region corresponding to the parotid gland or sublingual salivary gland. The asymptomatic, unilateral, radiolucent cavity configured by Stafne bone defect can be situated within posterior mandibular region between mandibular angle and third molar or below inferior dental canal and slightly superior to the inferior cortical mandibular border. Exceptionally, Stafne bone defect may engender expansion of the buccal cortex (Kaya et al., 2018; Hisatomi et al., 2019).

Stafne bone defect can be expounded as

- a bone cavity or depression situated upon lingual aspect of mandible adjacent to the inferior margin.
- a well demarcated, spherical, elliptical or occasionally lobulated radiolucency between one centimetre to 3 centimetres magnitude generally situated beneath inferior alveolar canal. The lesion is anterior to angle of mandible within the region of antegonial notch and fossa of submandibular salivary gland.
- a corticated, unilocular, radiolucency confined beneath the mandibular canal, between first molar and angle of mandible or exceptionally within buccal ramus or lingual ramus of the mandible.
- a developmental depression visualized along mesial aspect of mandible adjacent to the angle or anteriorly along the body.
- a non-corticated, well circumscribed, spherical or elliptical defect or pseudocyst situated within lingual surface of mandible, usually upon the mandibular angle or caudal to the mandibular canal. Occasionally, the lesion appears within anterior part of mandible. Intraoral, multiple or flanked, double Stafne bone defects may be observed within the mandible (Kaya et al., 2018; Hisatomi et al., 2019).

Figure 1: Stafne bone defect manifesting as a well-defined, spherical, mucosa-covered mandibular defect (14).

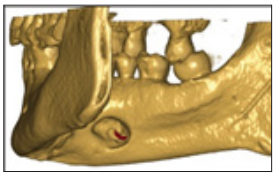

Figure 2: Stafne bone defect representing as a corticated, spherical depression within the mandible (15).

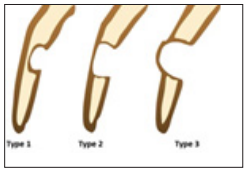

Figure 3 : Stafne bone defect delineating degrees and subtypes of mandibular bony excavation (16).

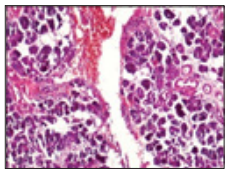

Figure 4: Stafne bone defect depicting a cavity imbued with aggregates and nests of salivary glands surrounded by connective tissue stroma (17).

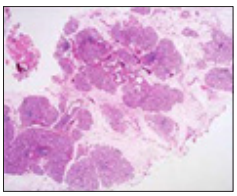

Figure 5: Stafne bone defect demonstrating lobules and aggregates of mucinous salivary glands enveloped within loose, fibroconnective tissue (18).

Figure 6: Stafne bone defect delineating a corticated, bony depression within the mandibular region (19).

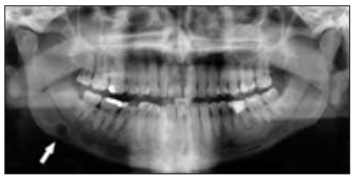

Figure 7: Stafne bone defect exhibiting a well-defined, spherical, radiolucent shadow confined to the mandible (19).

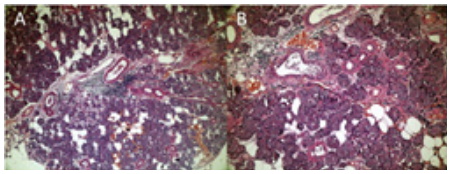

Figure 8: Stafne bone defect exemplifying aggregates and clusters of benign salivary glands enmeshed within a fibrous tissue stroma (20).

Differential Diagnosis: Stafne bone defect appearing adjacent or superior to inferior alveolar canal or adjoining apex of tooth requires a demarcation from asymptomatic, spherical or elliptical, well circumscribed, uniform, radiolucent lesions discernible upon radiographic examination of the mandible. Also, Stafne bone defect requires a segregation from various lytic lesions of the jaw (Hisatomi et al., 2017; Ozaki et al., 2015; Schneider et al., 2014).

Investigative Assay: Routine panoramic dental radiography is beneficial in initial discernment of the lesion. A consistent magnitude and radiographic appearance is pathognomonic of Stafne bone defect. Therefore, the lesion can be designated as a "static bone cyst". The defect may be discerned as an incidental feature during routine dental radiographic examination (Schneider et al., 2014; He et al., 2019; Ariji et al., 1993). Upon plain radiography, the bone defect manifests as a well-circumscribed, unilocular, spherical or elliptical, radiolucent defect of magnitude between one centimetre to three centimetres. Generally, the cyst is adjacent to inferior alveolar nerve and inferior border of posterior mandible,

impacted between molars and angle of jaw (He et al., 2019; Ariji et al., 1993; Lee et al., 2019). On conventional, panoramic radiography, the spherical or elliptical, uniform, radiolucent Stafne bone defect depicts a radiopaque perimeter within third molar region subjacent to the tooth roots (He et al., 2019; Ariji et al., 1993; Lee et al., 2019). The radiolucent defect may appear superimposed upon anterior, inferior teeth. Sometimes the defect may be palpable and interrupt the contour of inferior border of mandible (He et al., 2019; Ariji et al., 1993; Lee et al., 2019). The incidental Stafne bone defect manifests as a uniform, unilocular, spherical or elliptical, cystic, radiolucent lesion with a well defined perimeter. The lesion may be superior to or may encroach upon inferior alveolar nerve canal or upon inferior cortical border of the mandible or may project upon adjacent tooth's apex or may emerge within ramus of the mandible (He et al., 2019; Ariji et al., 1993; Lee et al., 2019). On account of exclusive location upon plain radiography, Stafne bone defect arising within posterior mandible may be effortlessly determined. However, imaging feature may vary and an appropriate assessment is required to evaluate and demarcate the bone defect from associated pathological intraosseous lesions (He et al., 2019; Ariji et al., 1993; Lee et al., 2019). Computerized tomography (CT) is beneficial in determining depth, extension and constituents of Stafne bone defect. Computerized tomography is necessitated for diagnosing debatable lesions upon panoramic radiographs or painful, oedematous or symptomatic lesions. Additionally, the defect can be correlated with neighbouring anatomical structures (Lee et al., 2019; Nishimura et al., 2018; Ozdede, 2020). Upon computerized tomography, a shallow defect circumscribed by a perimeter of cortical bone may peek through medial cortex of mandible. Soft tissue anomalies are absent although a segment of submandibular salivary gland may herniate into the defect (Lee et al., 2019; Nishimura et al., 2018; Ozdede, 2020). Computerized tomography can be utilized to assess magnitude of the bone defect and concurrence with mandibular lingual or buccal cortical plate (Lee et al., 2019; Nishimura et al., 2018; Ozdede, 2020).

The base of Stafne bone defect is categorized into subtype I, subtype II and subtype III contingent to concordance with buccal cortical plate and is defined as

- bony perimeter of the lesion designated as attenuated, dense or with the absence of bone sclerosis
- proportionate internal density of the lesion denominated as hypodense or hyper-dense •configuration as spherical or elliptical
- topographic concordance with base of the mandible
- interval to mandibular base (Lee et al., 2019; Nishimura et al., 2018; Ozdede, 2020).

Subtype I is frequently delineated wherein a dense, sclerotic, bony perimeter with a comprehensive outline is the chief radiographic feature. Intrinsic constituents of the defect appear hypodense. Lesion may be elliptical and frequently appear contiguous with inferior cortical mandibular line (Lee et al., 2019; Nishimura et al., 2018; Ozdede, 2020).

Occasionally, sialography may be adopted to demonstrate salivary gland tissue impacted within the bone. Sialography is advantageous in excluding associated lesions and assessing defects imbued with salivary gland tissue as the ductular configurations can be appropriately evaluated (Lee et al., 2019; Nishimura et al., 2018; Ozdede, 2020).

Magnetic Resonance Imaging (MRI) is beneficial in differentiating soft tissue content of the defect. Upon magnetic resonance imaging, contiguity of submandibular salivary gland with the mandibular bone defect may be observed (Lee et al., 2019; Nishimura et al., 2018; Ozdede, 2020).

References

1. Stafne, E. C. (1942). Bone cavities situated near the angle of the mandible. *J Am Dent Assoc, 29*(17), 1969–1972. DOI: https://doi.org/10.14219/jada.archive.1942.0315
2. Morita, L., Munhoz, L., Nagai, A. Y., Hisatomi, M., Asaumi, J. & Arita, E. S. (2021). Imaging features of Stafne bone defects on computed tomography: An assessment of 40 cases. *Imaging Sci Dent, 51*(1), 81-86. DOI: 10.5624/isd.20200253
3. Aps, J. K. M., Koelmeyer, N. & Yaqub, C. (2020). Stafne's bone cyst revisited and renamed: the benign mandibular concavity. *Dentomaxillofac Radiol, 49*(4), 20190475. DOI: 10.1259/dmfr.20190475
4. Kaya, M., Ugur, K. S., Dagli, E., Kurtaran, H. & Gunduz, M. (2018). Stafne bone cavity containing ectopic parotid gland. *Braz J Otorhinolaryngol, 84*(5), 669–672. DOI: https://doi.org/10.1016/j.bjorl.2016.02.004
5. Hisatomi, M., Munhoz, L., Asaumi, J. & Arita, E. S. (2019). Stafne bone defects radiographic features in panoramic radiographs: assessment of 91 cases. *Med Oral Patol Oral Cir Bucal, 24*(1), e12–e19. DOI:10.4317/medoral.22592
6. Hisatomi, M., Munhoz, L., Asaumi, J. & Arita, E. S. (2017). Parotid mandibular bone defect: a case report emphasizing imaging features in plain radiographs and magnetic resonance imaging. *Imaging Sci Dent, 47*(4):269–273. DOI: 10.5624/isd.2017.47.4.269
7. Ozaki, H., Ishikawa, S., Kitabatake, K., Yusa, K., Tachibana, H. & Lino, M. (2015). A case of simultaneous unilateral anterior and posterior Stafne bone defects. *Case Rep Dent*, 2015, 983956. DOI: 10.1155/2015/983956
8. Schneider, T., Filo, K., Locher, M. C., Gander, T., Metzler, P., Grätz, K. W., Kruse, A. L. & Lübbers, H. T. (2014). Stafne bone cavities: systematic algorithm for diagnosis derived from retrospective data over a 5-year period. *Br J Oral Maxillofac Surg, 52*(4), 369–374. DOI: 10.1016/j.bjoms.2014.01.017
9. He, J., Wang, J., Hu, Y. & Liu, W. (2019). Diagnosis and management of Stafne bone cavity with emphasis on unusual contents and location. *J Dent Sci, 14*(4), 435–439. DOI: 10.1016/j.jds.2019.06.001
10. Ariji, E., Fujiwara, N., Tabata, O., Nakayama, E., Kanda, S., Shiratsuchi, Y. & Oka, M. (1993). Stafne's bone cavity. Classification based on outline and content determined by computed tomography. *Oral Surg Oral Med Oral Pathol,*

76(3), 375–380. DOI: 10.1016/0030-4220(93)90271-5
11. Lee, K. C., Yoon, A. J., Philipone, E. M. & Peters, S. M. (2019). Stafne bone defect involving the ascending ramus. *J Craniofac Surg, 30*(4), e301–e303. DOI:10.1097/SCS.0000000000005252
12. Nishimura, S., Osawa, K., Tanaka, T., Imamura, Y., Kokuryo, S., Habu, M., Jyoujima, T., Miyamura, Y., Mochida, K. I., Inoue, T., Kito, S., Wakasugi-Sato, N., Matsumoto-Takeda, S., Oda, M., Yoshiga, D., Kodama, M., Sasaguri, M., Tominaga, K., Yoshioka, I. & Morimoto, Y. (2018). Multiple mandibular static bone depressions attached to the three major salivary glands. *Oral Radiol, 34*(3), 277–280. DOI: 10.1007/s11282-017-0304-x
13. Ozdede, M. (2020). An unusual case of double stafne bone cavities. *Surg Radiol Anat, 42*(5), 543–546. DOI:https://link.springer.com/article/10.1007/s00276-019-02403-8
14. Image 1 Courtesy: OOOO Journal
15. Image 2 Courtesy: J oral and maxillofacial radiology
16. Image 3 Courtesy: Imaging science in dentistry
17. Image 4 Courtesy: joomr.com
18. Image 5 Courtesy: jdras.org
19. Image 6 and 7 Courtesy: Wikipedia.com
20. Image 8 Courtesy: Science direct